JEBAT, 2024, Vol 7, No 2, 98-105
https://doi.org/10.54987/jebat.v7i2.1051

JOURNAL OF ENVIRONMENTAL BIOREMEDIATION AND TOXICOLOGY
Website: http://journal.hibiscuspublisher.com/index.php/JEBAT/index

Substrate Inhibition Kinetic Modelling of the Growth of *Bacillus* sp. Strain Neni-10 on Phenol

Rusnam[1]*, Fachri Ibrahim Nasution[1] and Hafeez Muhammad Yakasai[2]

[1]Department of Agricultural Engineering, Faculty of Agricultural Technology, Andalas University, Padang, 25163, Indonesia.
[2]Department of Biochemistry, Faculty of Basic Medical Sciences, College of Health Science, Bayero University, Kano, PMB 3011, Nigeria.

*Corresponding author:
Prof Dr. Rusnam
Department of Agricultural Engineering,
Faculty of Agricultural Technology,
Andalas University, Padang, 25163,
Indonesia.
Email: rusnam_ms@yahoo.com

HISTORY

Received: 14th Sep 2024
Received in revised form: 5th Dec 2024
Accepted: 24th Dec 2024

KEYWORDS

Substrate Inhibition Kinetics
Bioremediation
Phenol
Aiba
Bacillus sp.

ABSTRACT

Phenol is particularly harmful among the numerous xenobiotic compounds produced by the industry. A significant portion of the more than 1.5 million tons of sludge waste produced globally for industrial use consists of phenol and phenolic compounds, some of which are released into the environment without adequate safety assessment or control, leading to soil and water pollution. The potential use of phenol as a carbon source by many bacterial species can help mitigate phenol pollution through bioremediation of this hazardous material. This study employs several microbial growth kinetics models that govern the growth rate of a bacterium on phenol, with a focus on the comparative performance of the popular Haldane model alongside other models. The specific maximum growth rate (μ_m) was initially estimated using the no-lag modified logistics model. Among the kinetic models evaluated, the Aiba model exhibited the highest precision and accuracy, as demonstrated by statistical indices, including the lowest MPSD and AICc values, and bias and accuracy factors closest to 1. Despite variability in its parameter estimates, the Aiba model provided a meaningful kinetic description of phenol inhibition at high concentrations. Models such as Monod, Moser, Pamukoglu and Kargi, and Han-Levenspiel showed poor fitting. The maximum reduction rate, half-saturation constant for maximal reduction, and half-inhibition constant were the designated values of the Aiba constants, which were represented by (μ_m, K_s, and K_i) as 1.30±1.40 hr^{-1} (S.E.), 524.64±753.63 mg/L (S.E.), and 609.78±196.34 mg/L (S.E.), respectively. The results of curve fitting interpolation should not be regarded as the true value. The actual μ_{max} is defined as the point at which the slope's gradient reaches zero; in this case, it was determined to be 0.295 h^{-1} at a phenol concentration of 360 mg/L. This study highlights the advantages of employing substrate inhibition models, such as the Aiba and Haldane models, for accurately characterizing microbial growth in the presence of toxic xenobiotics, like phenol, especially for optimizing bioprocesses, such as wastewater treatment.

INTRODUCTION

The environment is chock-full of harmful chemicals, including phenol, that are hazardous to human health. Globally, industries generated more than 80,000 chemicals for industrial use, and even more compounds were released into the atmosphere without sufficient testing to ensure their safety [1]. Phenol is a unique and ubiquitous industrial pollutant, as well as a potentially hazardous chemical resulting directly from industrialization. The contamination of soils and water bodies by phenol has escalated throughout the years, immediately raising concerns over its removal from the environment [2]. Symptoms of acute phenol poisoning may result from inhalation of phenol or direct dermal exposure. Phenol poses significant irritant effects on the eyes, skin, and mucous membranes. The symptoms in humans include tachycardia, dyspnea, impaired coordination, tremors, syncope, and even coma at high concentrations. Other symptoms include irregular breathing patterns, tremors and muscle weakness, loss of equilibrium, convulsions, coma, and respiratory failure. Studies in rodents, including rats, mice, and rabbits, show elevated acute toxicity following oral exposure to phenol [3–6]. The Reference Dose for phenol was established at 0.6 mg/kg/day following studies on rats that indicated a reduction in fetal body weights. The reference dosage is an oral exposure evaluation for the general population, including sensitive subgroups, expected to have no appreciable risk of harmful non-cancerous effects during a lifetime. The reference dose is below the threshold at which cancer may arise. Increased exposures beyond the

reference dosage elevate the likelihood of adverse health effects. Prolonged exposure beyond the recommended dosage does not invariably preclude adverse health effects. The EPA possesses limited trust in the study utilized to establish the reference dose due to the administration method of gavage employed in that research. Nonetheless, the evidence encompasses multiple supplemental investigations (chronic, subchronic, and reproductive/developmental), leading the EPA to possess medium confidence in the reference dose overall [3,7–11].

The bioremediation process is currently the predominant treatment technology for phenol-laden wastewater globally, particularly at very low concentrations, and has attracted significant interest. Compared to physicochemical approaches, bioremediation offers numerous advantages, including a simple pre-treatment process, minimal initial equipment investment, high treatment capacity, sustainability, and the absence of secondary pollutants. Consequently, researchers must investigate bioremediation techniques for phenolic wastewater utilizing phenol-degrading microorganisms. A significant number of microorganisms capable of metabolizing phenol have been identified so far [12–19].

The optimization of biological transformation processes is constrained by the lack of readily available quantitative and mathematically processed or guided experimental data. Various mathematical models have been employed to simulate the metabolic characteristics of xenobiotics upon interaction with isolated microbial populations or pure microbial cultures. A valuable tool in bacterial growth in the presence of toxic chemicals is the relationship between the inhibitory impact of increased substrate concentration (S) and the maximum specific growth rate (μ_{max}) of the bacteria. The Monod equation is traditionally used as a common tool to characterize the relationship between growth and substrate consumption on nontoxic substrates [20,21]. Conversely, when a substrate inhibits its own biodegradation, the original Monod model demonstrates limited applicability. The development of new constant-carrying derivatives has occurred to enable substrate-related modifications.

The Haldane model represents substrate inhibition of growth or degradation rates and is prevalent in numerous published studies. Despite evidence indicating that alternative models exhibit greater accuracy when simultaneously considering numerous substrate-inhibiting chemicals, such as phenol, this model remains extensively utilized. The Haldane model is not the sole model presently accessible [22]. Other less-utilized models include Luong [23,24] and Edward [25]. In certain situations, the Haldane may become less optimal due to the adoption of more comprehensive models that are presently available. It is therefore inadvisable to utilize the Haldane model indiscriminately without conducting a thorough statistical analysis or error function analysis, and exploring alternative models using previously gathered data on growth or degradation rates. This study advances previous research by predicting the impact of substrate or phenol on bacterial growth rates through various substrate inhibition kinetic models.

MATERIALS AND METHODS

Data from primary modeling, especially the µm data from the growth of *Bacillus* sp. strain Neni-10 on phenol [28], were utilized in this study. The ten models of inhibition kinetics are shown in **Table 1**.

Table 1. Various mathematical models have been developed for degradation kinetics involving substrate inhibition of phenol in B. subtilis strain Neni-10.

Author	Degradation Rate	Author
Monod	$\frac{\mu_{max}S}{S+K_s}$	[26]
Haldane	$\frac{\mu_{max}S}{S+K_s+\left(\frac{S^2}{K_i}\right)}$	[27]
Pamukoglu and Kargi	$\frac{\mu_{max}S}{S+K_s+\left(\frac{S^m}{K_i}\right)}$	[28]
Teissier	$\mu_{max}\left(1-exp\left(-\frac{S}{K_i}\right)-exp\left(\frac{S}{K_s}\right)\right)$	[29]
Aiba	$\mu_{max}\frac{S}{K_s+S}exp\left(-\frac{S}{K_i}\right)$	[30]
Yano and Koga	$\frac{\mu_{max}S}{S+K_s+\left(\frac{S^2}{K_i}\right)\left(1+\frac{S}{K}\right)}$	[31]
Han and Levenspiel	$\mu_{max}\left(1-\left(\frac{S}{S_m}\right)\right)^n\left(\frac{S}{S+K_s\left(1-\left(\frac{S}{S_m}\right)\right)^m}\right)$	[32]
Luong	$\mu_{max}\frac{S}{S+K_s}\left(1-\left(\frac{S}{S_m}\right)\right)^n$	[33]
Moser	$\frac{\mu_{max}s^n}{K_s+s^n}$	[34]
Webb	$\frac{\mu_{max}S\left(1+\frac{S}{K}\right)}{S+K_s+\frac{S^2}{K_i}}$	[35]
Hinshelwood	$\mu_{max}\frac{S}{K_s+S}(1-K_pP)$	[36]

Note:
μ_{max} maximal specific growth rate
K_s half saturation constant
K_i inhibition constant
S_m maximal concentration of substrate tolerated
K_p product inhibition constant
m, n, K curve parameters
S substrate concentration
p product concentration

Fitting of the data

Fitting of the inhibition curves using various growth models was performed using the CurveExpert Professional software (Version 1.6) by nonlinear regression, utilizing the Marquardt algorithm.

Error function analyses

The error function tests for statistical discrimination utilized in this study are root-mean-squared error (RMSE), adjusted coefficient of determination (R^2) [37], HQ (Hannan and Quinn's Criterion) [38], Accuracy Factor (AF) and Bias Factor (BF) [39], Marquardt's percent standard deviation (MPSD) [40–42], corrected Akaike Information Criterion (AICc) [43,44], Bayesian Information Criterion (BIC) [45]. In general, *Obi* and *Pdi* represent the predicted and observed values, respectively, n is the total number of observations, and p is the total number of parameters in the model [46].

RMSE was calculated using the following formula;

$$RMSE = \sqrt{\frac{\sum_{i=1}^{n}(Pd_i - Ob_i)^2}{n-p}} \qquad \text{(Eqn. 1)}$$

BF and AF were calculated using the following formula;

$$Bias\ factor = 10\left(\sum_{i=1}^{n} log\frac{(Pd_i/Ob_i)}{n}\right) \quad \text{(Eqn. 2)}$$

$$Accuracy\ factor = 10\left(\sum_{i=1}^{n} log\frac{|(Pd_i/Ob_i)|}{n}\right) \quad \text{(Eqn. 3)}$$

AICc was calculated using the following formula;

$$AICc = 2p + n\ln\left(\frac{RSS}{n}\right) + \frac{2(p+1)+2(p+2)}{n-p-2} \quad \text{(Eqn. 4)}$$

BIC was calculated using the following formula;

$$BIC = n\mathrm{In}\left(\frac{RSS}{n}\right) + k\mathrm{In}(n) \quad \text{(Eqn. 5)}$$

HQC was calculated using the following formula;

$$HQC = nIn\left(\frac{RSS}{n}\right) + 2k\mathrm{In}(\mathrm{In}\ n) \quad \text{(Eqn. 6)}$$

Adjusted coefficient of determination (R^2) was calculated using the following formula;

$$Adjusted\ (R^2) = 1 - \frac{RMS}{S_Y^2} \quad \text{(Eqn. 7)}$$

$$Adjusted\ (R^2) = 1 - \frac{(1-R^2)(n-1)}{(n-p-1)} \quad \text{(Eqn. 8)}$$

MPSD was calculated using the following formula;

$$MPSD = 100\sqrt{\frac{1}{n-p}\sum_{i=1}^{n}\left(\frac{Ob_i - Pd_i}{Ob_i}\right)^2} \quad \text{(Eqn. 9)}$$

RESULTS AND DISCUSSION

The results of the RMSE, AICc, adjustedR^2, F-test, and bias and accuracy factor comparisons demonstrate that the Aiba model is the most accurate and precise of the kinetic models considered (**Table 2**). The Aiba model exhibited the lowest values for MPSD, AICcc, HQC, BIC, RMSE and adjR^2, BF, and AF, closest to 1, and was the second-best model based on the rest of the error function scores. The resultant fittings (**Figs. 1 to 9)** demonstrate a satisfactory fit, except for the Luong, Moser, Monod, Pamukoglu, and Kargi and Han Levenspiel models.

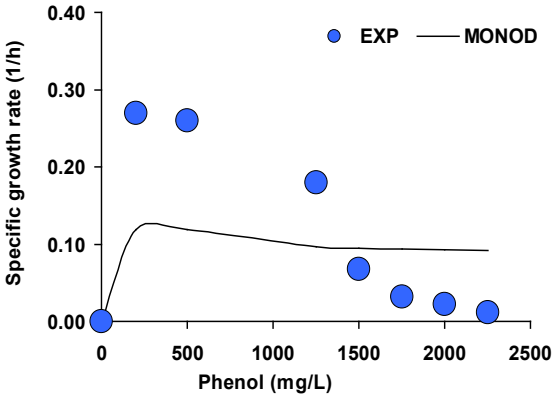

Fig 2. The growth data as fitted concerning phenol concentration using the model of Monod.

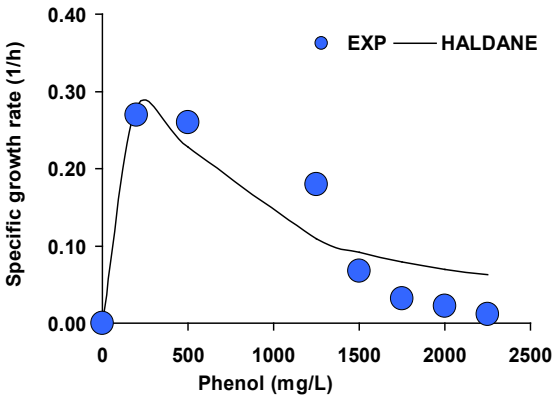

Fig 3. The growth data as fitted with respect to phenol concentration using the model of Haldane.

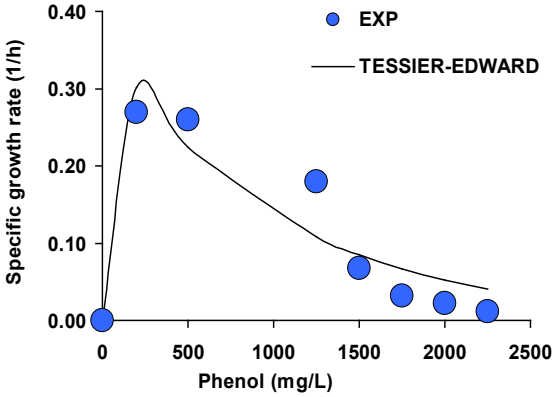

Fig 4. The growth data as fitted with respect to phenol concentration using the model of Teissier.

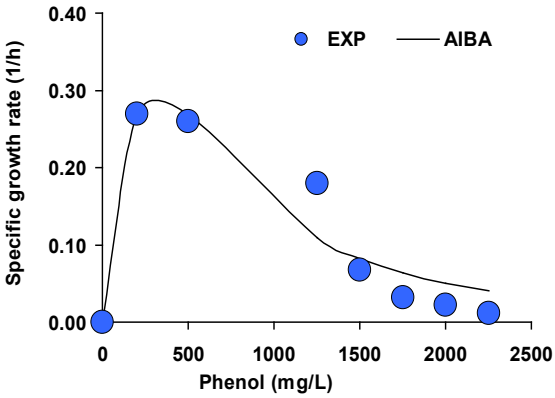

Fig 5. The growth data as fitted with respect to phenol concentration using the model of Aiba.

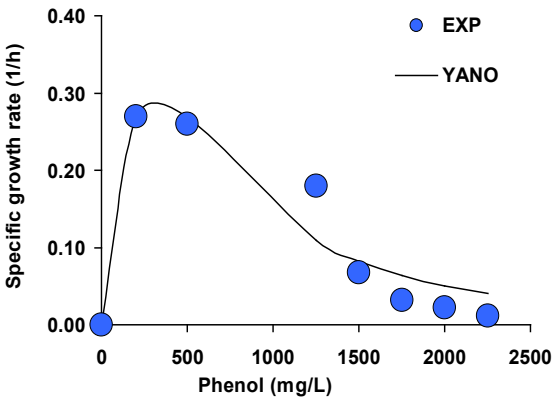

Fig 6. The growth data as fitted with respect to phenol concentration using the model of Yano and Koga.

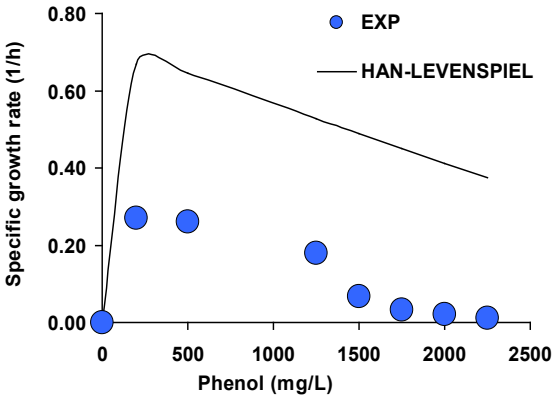

Fig 7. The growth data as fitted with respect to phenol concentration using the model of Han and Levenspiel.

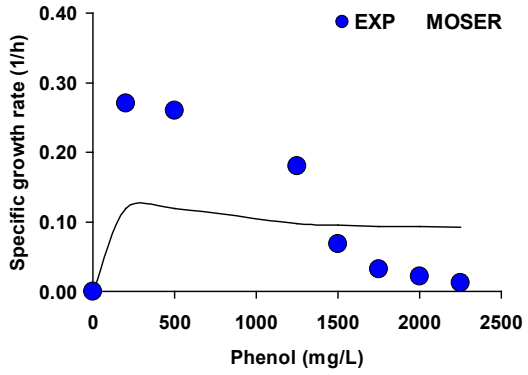

Fig 8. The growth data as fitted with respect to phenol concentration using the model of Moser.

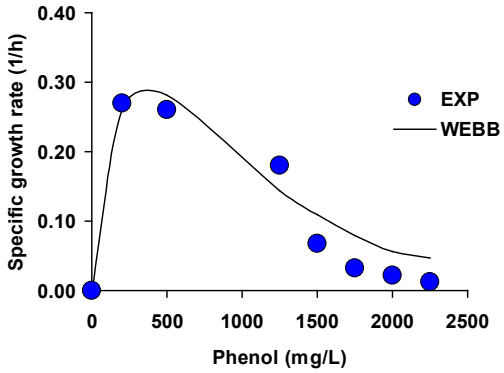

Fig 9. The growth data as fitted with respect to phenol concentration using the model of Webb.

Table 2. Statistical analysis of the various fitting models.

Model	p	RMSE	adR²	MPSD	AICc	BIC	HQC	BF	AF
Luong	4	0.212	n.a.	n.a.	n.a.	n.a.	n.a.	n.a.	n.a.
Yano	4	0.045	0.74	61.50	-7.335	-47.017	-49.478	1.362	1.545
Tessier-Edward	3	0.046	0.74	56.84	-25.700	-46.795	-48.641	1.363	1.607
Aiba	3	0.034	0.87	44.48	-30.698	-51.793	-53.639	1.248	1.397
Haldane	3	0.053	0.59	63.05	-23.563	-44.658	-46.504	1.534	1.796
Monod	2	0.104	-8.26	96.47	-22.450	-34.291	-35.522	1.396	2.430
Han and Levenspiel	5	0.596	-11.3	123.61	89.865	-5.738	-8.814	5.669	5.669
Moser	3	0.093	-13.0	169.91	-14.388	-35.483	-37.329	1.127	2.540
Hinshlewood	4	0.141	-2.7	13451	11.081	-28.601	-31.062	0.925	1.567
Webb	4	0.042	0.77	60.99	-8.324	-48.007	-50.468	1.547	1.651

Note:
p no of parameters
RMSE Root Mean Square Error
AdjR² Adjusted Coefficient of determination
MPSD Marquardt's percent standard deviation
BF Bias factor
AF Accuracy factor
n.a. not available

Maximum reduction rate, half saturation constant for maximal reduction, and half inhibition constant were the designated values of the Aiba constants, which are represented by μ_{max}, K_s, and K_i were 1.30±1.40 hr^{-1} (S.E. or Standard error), 524.64±753.63 mg/L (S.E.), and 609.78±196.34 mg/L (S.E.), respectively. The results of curve fitting interpolation should not be regarded as the true value. The actual μ_{max} is defined as the point at which the slope's gradient reaches zero; in this case, it was determined to be 0.295 h^{-1} at a phenol concentration of 360 mg/L. The equation for the Aiba model, utilizing the values derived from the fitting, is presented as follows;

$$\mu_m = 1.30 \frac{S}{524.64 + S} exp\left(-\frac{S}{609.78}\right)$$

Models such as those proposed by Luong, Teissier, and Hans Levenspiel have been established to address scenarios where the growth rate approaches zero at elevated substrate concentrations, a limitation of the earlier Monod model.

Excessive substrate concentrations can exert toxic and inhibitory effects on microbial growth. The current application of the Haldane model for assessing the impact of toxic xenobiotics on xenobiotic-degrading bacteria primarily focuses on phenol-degrading microorganisms. This is subsequently referenced by Teissier. Other models were found to be less frequently reported, primarily because, in many instances, only the Haldane model was employed to assess the impact of phenol on the growth or degradation rate of microorganisms in phenol [47,48,48–50]. In 1930, Haldane introduced his model, which is now referred to as the Haldane model.

The model is considered an advancement of the Monod model. The model incorporates a third constant, Ki, to address the inhibition of the specific growth rate that is dependent on substrate concentration. The substrate concentration corresponding to a specific growth rate that is half of the maximum growth rate, in the absence of inhibition, is defined as the inhibition constant, or Ks. High concentrations of hazardous substrates may impede the specific growth rate of an organism. The model is capable of handling both hazardous and non-hazardous substrates. The Haldane model effectively characterizes all stages of growth rate kinetics. The Haldane model was extensively employed due to its effective representation of growth rates across both low and high substrate concentrations. Prior to the widespread adoption of the Haldane model, the classical Monod model was the most frequently employed model.

In 1942, Jacques Monod introduced the Monod model to elucidate the relationship between specific growth rate and substrate consumption rate in a bioreactor. The Michaelis-Menten equation and the Monod equation, although similar in appearance, are grounded in theoretical frameworks rather than empirical observations [26]. The Monod equation for the specific growth rate parallels the Michaelis-Menten expression for enzyme kinetics and can be articulated using constants. The methods provided for calculating v_{max} and K_m in enzyme reactions can theoretically be applied to determine μ_{max} and K_S as well. The model can be defined in its various versions using substrate concentration alone or in conjunction with biomass concentration. X represents biomass concentration, K_s denotes the half-saturation constant, the specific bacterial growth rate is indicated, and μ_{max} refers to the maximum bacterial growth rate. The maximum growth rate and the half-saturation constant of bacteria remain unchanged. The Monod model in the bioreactor assumes the presence of a single substrate that limits growth.

The Monod model has several limitations regarding its applicability as a model [51]. At elevated substrate concentrations, the initial restriction becomes evident. The maximum specific growth rate remains unaffected by substrate concentration at elevated levels. A second restriction arises under conditions of low substrate concentration. Growth at low substrate concentrations is contingent upon the specific substrate utilized. The Monod model is not applicable in the presence of substrate inhibition [29,32,52]. Analogous to the Michaelis-Menten kinetics model, at low substrate concentrations, the growth rate exhibits first-order behavior with respect to substrate concentrations, whereas at high substrate concentrations, the growth rate demonstrates zero-order behavior with respect to substrate concentrations. The Haldane model and various substrates exhibit inhibition at elevated substrate concentrations, as evidenced by the negative slope of the growth rate, indicating a negative order of reaction. In numerous xenobiotics or hazardous compounds, bioremediation is effective; however, toxic substrates that inhibit bacterial growth and substrate consumption render the Monod models ineffective, necessitating the use of alternative substrate inhibition models [53–57]. The Aiba model is the second-most popular model, after the Haldane model, and it recognizes the substrate inhibition model, which illustrates microbial growth under inhibitory substrate concentrations (**Table 3**). The Aiba model is frequently applicable in bioprocesses involving growth on hazardous compounds, including phenol. The classical or traditional Monod model posits that increased substrate availability enhances microbial growth until saturation is attained. The Aiba model, on the other hand, posits that excessive substrate may inhibit microbial activity, providing a more accurate depiction of scenarios where substrate toxicity constrains microbial function, especially when grown on toxic substrates. The model describes microbial growth that initially increases with substrate concentration, but at high substrate concentrations, it will decline due to inhibition after a specific threshold concentration. The exponential inhibition term describes or models the extent to which elevated substrate concentrations diminish microbial activity. The Aiba model, like the Haldane model, is predicated on the interaction between enzymes and substrates.

The Aiba model has been utilized to model substrate inhibition kinetics of numerous microbial bioprocesses [71–80], and will continue to find utility after the Haldane model. It has been extensively utilized in modeling wastewater treatment, particularly when the growth rate of phenol- or other xenobiotic-degrading bacteria is diminished at elevated substrate concentrations. The model is beneficial in fermentation processes, bioengineering, and process control, as it helps understand how substrates behave at specific concentrations and how to determine the optimal substrate quantities to manage their toxicity, thereby improving treatment effectiveness and microbial consistency.

CONCLUSION

In this work, we found that the growth rate of *Baccillus* sp. strain Neni-10 was significantly impeded at exceedingly high concentrations of phen*ol,* and the Aiba model demonstrated strong utility in describing microbial growth inhibition at elevated phenol concentrations. Its exponential inhibition term effectively captured the decline in specific growth rate due to substrate toxicity, a limitation of the classical Monod model. While the Haldane model remains the most robust and widely applied for xenobiotic biodegradation, the Aiba model offers a valuable alternative for modeling systems where phenol acts as both substrate and inhibitor. Its future applications in bioreactor optimization and wastewater treatment systems underline its relevance in environmental biotechnology. In general, both models enhance our ability to understand and predict microbial behavior under inhibitory substrate conditions, thereby allowing for improved process control and environmental remediation strategies.

Note on Use of AI Tools

The authors utilized various computer tools to assist in writing and reviewing this manuscript. ChatGPT (by OpenAI) was used to help organize ideas, explain scientific terms more clearly, and write better sentences. Grammarly helped to correct grammar and spelling mistakes. QuillBot was used to rephrase some sentences and make them easier to read. All the writing produced by these tools was carefully reviewed and edited by the authors. The authors ensured that all information is accurate and adheres to academic standards. The authors are fully responsible for everything written in this paper, including the results and conclusions.

Table 3. A summary of selected secondary modelling of the best models and kinetic parameters governing the phenol-degrading bacterium.

Microorganism	Best Model	Temp °C	Max phenol	μ_{max} (h^{-1})	K_s (mgL^{-1})	K_i (mgL^{-1})	S_m, K_1 or K_2 (mgL^{-1})	Reference
Pseudomonas putida	Haldane	26±0.5	500	0.436	6.19	54.1	-	[58]
Rhodococcus AQ5NOL1	Haldane	35	1110	0.11	99.03	354	-	[22]
Pseudomonas putida	Haldane	30	-	0.569	18.539	99.374	-	[59]
Mixed consortium	Han-Levenspiel	27	800	0.4029	110.93		790	[60]
Pseudomonas sp.	Haldane	29±2	400	0.0324	0.0324	0.0324	-	[61]
Pseudomonas sp.	Luong	29±2	400	0.0238	0.0238	-	400	[61]
Mixed bacterial culture	Luong	30	350	1.04	153.2	-	540	[23]
Bacillus cereus MTCC 9817	Luong	30	-	0.755	925.8	-	1859.3	[62]
Pseudomonas IES-Ps-1	Luong	35	2000	0.38	111	-	2000	[63]
Pseudomonas IES-S	Luong	35	2000	0.63	77	-	2174	[63]
Basillus IES-B	Luong	35	2000	1.2	102	-	2190	[63]
Pseudomonas fluorescence	Haldane	30	-	0.229	0.374		729	[64]
Pseudomonas fluorescence	Yano and Koga	30	-	0.229	0.377	-	411	[64]
Pseudomonas fluorescence	Aiba	30	-	0.229	0.376		2008	[64]
Sulfolobus solfataricus 98/2	Haldane	80	-	0.094	77.7	319.4	93	[65]
Candida tropicalis PHB5	Haldane	30	2,400	0.3407	15.81	169.0	-	[66]
Mixed consortium of bacteria	Haldane	30	800	0.1301	99.84	220.9	-	[67]
Alcaligenes faecalis B6-2	Haldane	30	1410	0.48	188.16	469.23	297.1	[68]
Alcaligenes faecalis B8-1	Haldane	30	1410	0.14	32.85	447.44	121.2	[68]
Alcaligenes faecalis D3-1	Haldane	30	1410	0.38	267.3	1847.82	702.8	[68]
Acinetobacter johnsonii D1	Haldane	30	1410	0.55	483.83	2582.63	1117.8	[68]
Pseudomonas citronellolis PDB16	Edwards	35 to 37	1200	0.385	132.91	507.58	-	[69]
Candida tropicalis PHB5	First-order (PBR)	30	2400	-	-	-	-	[70]
Pseudomonas fredriksbergensis	Haldane	28	700	0.062	11	121	-	[71]
Rhodococcus sp. Strain SKC	Haldane	30	1500	0.3	36.40	418.79		[72]
Rhodococcus ruber C1	Haldane	40	2000	1.527	69.74	4895		[73]
Comamonas testosteroni strain F4	Not available	30	1000	-	-	-		[74]
Bacillus sp. Strain Neni-10	Aiba	30	2000	1.30	524.64	609.78		This study

REFERENCES

1. Özkara A, Akyil D, Konuk M. Pesticides, Environmental Pollution, and Health. In: Larramendy M, Soloneski S, editors. Environmental Health Risk - Hazardous Factors to Living Species [Internet]. InTech; 2016 [cited 2020 July 17]. Available from: http://www.intechopen.com/books/environmental-health-risk-hazardous-factors-to-living-species/pesticides-environmental-pollution-and-health
2. Ayeni O. A preliminary assessment of phenol contamination of Isebo River in south-western Nigeria. Greener J Phys Sci. 2014;4(2):30–7.
3. Bruce RM, Santodonato J, Neal MW. Summary Review of the Health Effects Associated With Phenol. Toxicol Ind Health. 1987 Oct 1;3(4):535–68.
4. Strikwold M, Spenkelink B, Woutersen RA, Rietjens IMCM, Punt A. Combining in vitro embryotoxicity data with physiologically based kinetic (PBK) modelling to define in vivo dose–response curves for developmental toxicity of phenol in rat and human. Arch Toxicol. 2013 Sept 1;87(9):1709–23.
5. Kottuparambil S, Kim YJ, Choi H, Kim MS, Park A, Park J, et al. A rapid phenol toxicity test based on photosynthesis and movement of the freshwater flagellate, Euglena agilis Carter. Aquat Toxicol. 2014 Oct 1;155:9–14.
6. Mohanta VL, Mishra BK. Occurrence and fate of phenolic compounds in groundwater and their associated risks. In: Legacy, Pathogenic and Emerging Contaminants in the Environment. CRC Press; 2021.
7. Kim JS, Chin P. Acute and chronic toxicity of phenol to mysid, Archaeomysis kokuboi. Korean J Fish Aquat Sci. 1995;28(1):87–97.

8. Abd Gami A, Shukor A, Yunus M, Abdul Khalil K, Dahalan FA, Khalid A, et al. Phenol and phenolic compounds toxicity. J Environ Microbiol Toxicol. 2014;2(1):11–23.
9. Gami AA, Shukor MY, Khalil KA, Dahalan FA, Khalid A, Ahmad SA. Phenol and its toxicity. J Environ Microbiol Toxicol. 2014;2(1):11–23.
10. Dhatwalia VK, Nanda M. Biodegradation of phenol: Mechanisms and applications. Toxicity and Waste Management Using Bioremediation. 2015. 198–214 p.
11. Duan W, Meng F, Cui H, Lin Y, Wang G, Wu J. Ecotoxicity of phenol and cresols to aquatic organisms: A review. Ecotoxicol Environ Saf. 2018;157:441–56.
12. Kujur RRA, Das SK. Pseudomonas phenolilytica sp. nov., a novel phenol-degrading bacterium. Arch Microbiol. 2022 May 14;204(6):320.
13. Rusnam, Gusmanizar N, Rahman MF, Yasid NA. Characterization of a Molybdenum-reducing and Phenol-degrading Pseudomonas sp. strain Neni-4 from soils in West Sumatera, Indonesia. Bull Environ Sci Sustain Manag E-ISSN 2716-5353. 2022 July 31;6(1):1–8.
14. Hanafee N, Salleh NAM, Ahmad SA, Saada WZ, Yusof MT. Characterization of phenol-degrading fungi isolated from industrial waste water in Malaysia. Asia-Pac J Mol Biol Biotechnol. 2019;27(2):35–43.
15. Aisami A, Yasid NA, Johari WLW, Shukor MY. Estimation of the Q10 value; the temperature coefficient for the growth of *Pseudomonas* sp. aq5-04 on phenol. Bioremediation Sci Technol Res. 2017 July 31;5(1):24–6.
16. Szilveszter S, Fikó DR, Máthé I, Felföldi T, Ráduly B. Kinetic characterization of a new phenol degrading Acinetobacter towneri strain isolated from landfill leachate treating bioreactor. World J Microbiol Biotechnol. 2023 Jan 17;39(3):79.
17. Mousa A. Isolation and Characterization of Phenol degrading Bacteria from Wastewater. Int J Biol Phys Chem Stud. 2023 Sept 10;5:17–24.
18. Bandi SS, Mallisetty R, Veluru S, Hamzah HT, Poiba VR, Srikanth R. Isolation, identification and optimization of potential phenol degrading bacterial strain P7 using Gen III microlog. AIP Conf Proc. 2023 Sept 13;2764(1):020007.
19. Sandhyarani R, Mishra S. Isolation and characterization of phenol degrading organism, optimization using doehlert design. Desalination Water Treat. 2019;148:351–62.
20. Kiviharju K, Salonen K, Leisola M, Eerikäinen T. Modeling and simulation of Streptomyces peucetius var. caesius N47 cultivation and ε-rhodomycinone production with kinetic equations and neural networks. J Biotechnol. 2006;126(3):365–73.
21. Shokrollahzadeh S, Bonakdarpour B, Vahabzadeh F, Sanati M. Growth kinetics and Pho84 phosphate transporter activity of Saccharomyces cerevisiae under phosphate-limited conditions. J Ind Microbiol Biotechnol. 2007;34(1):17–25.
22. Arif NM, Ahmad SA, Syed MA, Shukor MY. Isolation and characterization of a phenol-degrading *Rhodococcus* sp. strain AQ5NOL 2 KCTC 11961BP. J Basic Microbiol. 2013;53(1):9–19.
23. Hamitouche AE, Bendjama Z, Amrane A, Kaouah F, Hamane D. Relevance of the Luong model to describe the biodegradation of phenol by mixed culture in a batch reactor. Ann Microbiol. 2012;62(2):581–6.
24. Nickzad A, Mogharei A, Monazzami A, Jamshidian H, Vahabzadeh F. Biodegradation of phenol by Ralstonia eutropha in a Kissiris-immobilized cell bioreactor. Water Environ Res. 2012;84(8):626–34.
25. Saravanan P, Pakshirajan K, Saha P. Batch growth kinetics of an indigenous mixed microbial culture utilizing m-cresol as the sole carbon source. J Hazard Mater. 2009;162(1):476–81.
26. Monod J. The Growth of Bacterial Cultures. Annu Rev Microbiol. 1949;3(1):371–94.
27. Boon B, Laudelout H. Kinetics of nitrite oxidation by Nitrobacter winogradskyi. Biochem J. 1962;85:440–7.
28. Pamukoglu MY, Kargi F. Elimination of Cu(II) toxicity by powdered waste sludge (PWS) addition to an activated sludge unit treating Cu(II) containing synthetic wastewater. J Hazard Mater. 2007 Sept 5;148(1):274–80.
29. Teissier G. Growth of bacterial populations and the available substrate concentration. Rev Sci Instrum. 1942;3208:209–14.
30. Aiba S, Shoda M, Nagatani M. Kinetics of product inhibition in alcohol fermentation. Biotechnol Bioeng. 1968 Nov 1;10(6):845–64.
31. Yano T, Koga S. Dynamic behavior of the chemostat subject to substrate inhibition. Biotechnol Bioeng. 1969 Mar 1;11(2):139–53.
32. Han K, Levenspiel O. Extended Monod kinetics for substrate, product, and cell inhibition. Biotechnol Bioeng. 1988;32(4):430–7.
33. Luong JHT. Generalization of monod kinetics for analysis of growth data with substrate inhibition. Biotechnol Bioeng. 1987;29(2):242–8.
34. Moser A. Kinetics of batch fermentations. In: Rehm HJ, Reed G, editors. Biotechnology. VCH Verlagsgesellschaft mbH, Weinheim; 1985. p. 243–83.
35. Webb JLeyden. Enzyme and metabolic inhibitors [Internet]. New York: Academic Press; 1963. 984 p. Available from: https://www.biodiversitylibrary.org/bibliography/7320
36. Hinshelwood CN. The chemical kinetics of the bacterial cell. Clarendon Press, Gloucestershire, UK; 1946.
37. Ezekiel M. The Sampling Variability of Linear and Curvilinear Regressions: A First Approximation to the Reliability of the Results Secured by the Graphic "Successive Approximation" Method. Ann Math Stat. 1930;1(4):275–333.
38. Hannan EJ, Quinn BG. The Determination of the Order of an Autoregression. J R Stat Soc Ser B Methodol. 1979;41(2):190–5.
39. Ross T. Indices for performance evaluation of predictive models in food microbiology. J Appl Bacteriol. 1996;81(5):501–8.
40. Marquardt DW. An Algorithm for Least-Squares Estimation of Nonlinear Parameters. J Soc Ind Appl Math. 1963;11(2):431–41.
41. Seidel A, Gelbin D. On applying the ideal adsorbed solution theory to multicomponent adsorption equilibria of dissolved organic components on activated carbon. Chem Eng Sci. 1988 Jan 1;43(1):79–88.
42. Porter JF, McKay G, Choy KH. The prediction of sorption from a binary mixture of acidic dyes using single- and mixed-isotherm variants of the ideal adsorbed solute theory. Chem Eng Sci. 1999;54(24):5863–85.
43. Akaike H. A New Look at the Statistical Model Identification. IEEE Trans Autom Control. 1974;19(6):716–23.
44. Burnham KP, Anderson DR. Multimodel inference: Understanding AIC and BIC in model selection. Sociol Methods Res. 2004;33(2):261–304.
45. Schwarz G. Estimating the Dimension of a Model. Ann Stat. 1978;6(2):461–4.
46. Motulsky HJ, Ransnas LA. Fitting curves to data using nonlinear regression: a practical and nonmathematical review. FASEB J. 1987;1(5):365–74.
47. Agarry SE, Solomon BO. Kinetics of batch microbial degradation of phenols by indigenous *Pseudomonas fluorescence*. Int J Environ Sci Technol. 2008;5(2):223–32.
48. Agarry SE, Solomon BO, Layokun SK. Substrate inhibition kinetics of phenol degradation by binary mixed culture of *Pseudomonas aeruginosa* and *Pseudomonas fluorescence* from steady state and wash- out data. Afr J Biotechnol. 2008;7(21):3927–33.
49. Begum SS, Radha KV. Investigating the performance of inverse fluidized bed biofilm reactor for phenol biodegradation using *Pseudomonas fluorescence*. In: Proceedings of the International Conference on Green Technology and Environmental Conservation, GTEC-2011. 2011. p. 130–6.
50. Halmi MIE, Shukor MS, Johari WLW, Shukor MY. Mathematical modelling of the degradation kinetics of *Bacillus cereus* grown on phenol. J Environ Bioremediation Toxicol. 2014;2(1):1–5.
51. Kong JD. Modeling Microbial Dynamics: Effects on Environmental and Human Health [Internet] [PhD Thesis]. [Canada]: University of Alberta; 2017 [cited 2023 Nov 11]. Available from: https://era.library.ualberta.ca/items/0191844e-958e-49fb-bc42-feec802a29ea/view/b06920dd-a80e-427e-b7b9-4aa9433c579e/Kong_Jude_D_201708_PhD.pdf
52. Mulchandani A, Luong JHT, Groom C. Substrate inhibition kinetics for microbial growth and synthesis of poly-β-hydroxybutyric acid by *Alcaligenes eutrophus* ATCC 17697. Appl Microbiol Biotechnol. 1989;30(1):11–7.
53. Yakasai HM, Babandi A, Uba G. Inhibition Kinetics Study of Molybdenum Reduction by *Pantoea* sp. strain HMY-P4. J Environ Microbiol Toxicol. 2020 Dec 31;8(2):24–9.

54. Yakasai HM, Babandi A, Manogaran M. Modelling the Kinetics Molybdenum Reduction Rate by *Morganella* sp. J Environ Microbiol Toxicol. 2020 Dec 31;8(2):18–23.
55. Uba G, Abubakar A, Ibrahim S. Optimization of Process Conditions for Effective Degradation of Azo Blue Dye by Streptomyces sp. DJP15: A Secondary Modelling Approac. Bull Environ Sci Sustain Manag. 2021 Dec 31;5(2):28–32.
56. Othman AR, Rahim MBHA. Modelling the Growth Inhibition Kinetics of Rhodotorula sp. strain MBH23 (KCTC 11960BP) on Acrylamide. Bioremediation Sci Technol Res. 2019 Dec 28;7(2):20–5.
57. Habibi A, Vahabzadeh F. Degradation of formaldehyde at high concentrations by phenol-adapted *Ralstonia eutropha* closely related to pink-pigmented facultative methylotrophs. J Environ Sci Health - Part ToxicHazardous Subst Environ Eng. 2013;48(3):279–92.
58. Monteiro ÁAMG, Boaventura RAR, Rodrigues AE. Phenol biodegradation by *Pseudomonas putida* DSM 548 in a batch reactor. Biochem Eng J. 2000 Aug 1;6(1):45–9.
59. Şeker Ş, Beyenal H, Salih B, Tanyolaç A. Multi-substrate growth kinetics of *Pseudomonas putida* for phenol removal. Appl Microbiol Biotechnol. 1997;47(5):610–4.
60. Saravanan P, Pakshirajan K, Saha P. Growth kinetics of an indigenous mixed microbial consortium during phenol degradation in a batch reactor. Bioresour Technol. 2008;99(1):205–9.
61. Saravanan P, Pakshirajan K, Saha P. Kinetics of phenol degradation and growth of predominant Pseudomonas species in a simple batch stirred tank reactor. Bulg Chem Commun. 2011;43(4):502–9.
62. Halmi MIE, Shukor MS, Johari WLW, Shukor MY. Mathematical modeling of the growth kinetics of *Bacillus* sp. on tannery effluent containing chromate. J Environ Bioremediation Toxicol. 2014;2(1):6–10.
63. Hasan SA, Jabeen S. Degradation kinetics and pathway of phenol by *Pseudomonas* and *Bacillus* species. Biotechnol Biotechnol Equip. 2015;29(1):45–53.
64. Agarry SE, Audu TOK, Solomon BO. Substrate inhibition kinetics of phenol degradation by *Pseudomonas fluorescence* from steady state and wash-out data. Int J Environ Sci Technol. 2009;6(3):443–50.
65. Christen P, Vega A, Casalot L, Simon G, Auria R. Kinetics of aerobic phenol biodegradation by the acidophilic and hyperthermophilic archaeon *Sulfolobus solfataricus* 98/2. Biochem Eng J. 2012;62:56–61.
66. Basak B, Bhunia B, Dutta S, Chakraborty S, Dey A. Kinetics of phenol biodegradation at high concentration by a metabolically versatile isolated yeast *Candida tropicalis* PHB5. Environ Sci Pollut Res. 2014;21(2):1444–54.
67. Chakraborty B, Ray L, Basu S. Study of phenol biodegradation by an indigenous mixed consortium of bacteria. Indian J Chem Technol. 2015;22(5):227–33.
68. Heilbuth NM, Linardi VR, Monteiro AS, da RRA, Mimim LA, Santos VL. Estimation of kinetic parameters of phenol degradation by bacteria isolated from activated sludge using a genetic algorithm. J Chem Technol Biotechnol. 2015;90(11):2066–75.
69. Nandi L, Panigrahi AK, Maitra N, Chattopadhyay AP, Manna SK. Isolation, characterization and growth kinetics of phenol hyper-tolerant bacteria from sewage-fed aquaculture system. J Environ Sci Health Part A. 2020 Mar 20;55(4):333–44.
70. Basak B, Jeon BH, Kurade MB, Saratale GD, Bhunia B, Chatterjee PK, et al. Biodegradation of high concentration phenol using sugarcane bagasse immobilized *Candida tropicalis* PHB5 in a packed-bed column reactor. Ecotoxicol Environ Saf. 2019 Sept 30;180:317–25.
71. Aljbour SH, Khleifat KM, Tarawneh AA, Asasfeh B, Qaralleh H, El-Hasan T, et al. Growth Kinetics and Toxicity of Pseudomonas fredriksbergsis Grown on Phenol as Sole Carbon Source. J Ecol Eng. 2021;22(10):251–63.
72. Wen Y, Li C, Song X, Yang Y. Biodegradation of phenol by rhodococcus sp. Strain SKC: Characterization and kinetics study. Molecules. 2020;25(16).
73. Zhao T, Gao Y, Yu T, Zhang Y, Zhang Z, Zhang L, et al. Biodegradation of phenol by a highly tolerant strain *Rhodococcus ruber* C1: Biochemical characterization and comparative genome analysis. Ecotoxicol Environ Saf. 2021 Jan 15;208:111709.
74. Mortazavi A, Hassanshahian M, Ali E, Fenjan MN, Alawadi A, Alsalamy A. Isolation and Identification of Phenol-Degrading Bacteria from Iranian Soil and Leaf Samples. Front Biosci-Elite. 2023 Dec 12;15(4):29.